Solution-phase deposition and nanopatterning of GeSbSe phase-change materials

DELIA J. MILLIRON[1]*, SIMONE RAOUX[1], ROBERT M. SHELBY[1] AND JEAN JORDAN-SWEET[2]

[1] IBM Almaden Research Center, 650 Harry Road, San Jose, California 95120, USA
[2] IBM Watson Research Center, 1101 Kitchawan Road, Yorktown Heights, New York 10598, USA
*e-mail: milliron@us.ibm.com

Chalcogenide films with reversible amorphous–crystalline phase transitions have been commercialized as optically rewritable data-storage media[1,2], and intensive effort is now focused on integrating them into electrically addressed non-volatile memory devices (phase-change random-access memory or PCRAM)[3–5]. Although optical data storage is accomplished by laser-induced heating of continuous films, electronic memory requires integration of discrete nanoscale phase-change material features with read/write electronics. Currently, phase-change films are most commonly deposited by sputter deposition, and patterned by conventional lithography[3]. Metal chalcogenide films for transistor applications have recently been deposited by a low-temperature, solution-phase route[6–9]. Here, we extend this methodology to prepare thin films and nanostructures of GeSbSe phase-change materials. We report the ready tuneability of phase-change properties in GeSbSe films through composition variation achieved by combining novel precursors in solution. Rapid, submicrosecond phase switching is observed by laser-pulse annealing. We also demonstrate that prepatterned holes can be filled to fabricate phase-change nanostructures from hundreds down to tens of nanometres in size, offering enhanced flexibility in fabricating PCRAM devices with reduced current requirements.

The most widely studied material for phase-change data storage is $Ge_2Sb_2Te_5$ (refs 10,11), though a wide range of materials have been recently investigated in pursuit of greater phase stability and reduced power consumption during electrical switching[12–14]. Phase-change characteristics can be tuned through composition variation and doping to achieve sufficient amorphous-state stability for data retention while writing a bit as quickly as possible[12,15,16]. Crystallization behaviour of amorphous $SbSe_x$ alloy films has been investigated for optical-recording applications[15–17], and electrical switching was observed in amorphous Sb_2Se_3 over a decade ago[18]. Recently, $SbSe_x$ alloys have attracted renewed attention as potential PCRAM materials due to their relatively low melting temperatures, which reduce the power required to reset the material to the amorphous state[12]. Here, we report a solution-phase route to $SbSe_x$ materials that maintains the ability to alter composition and doping to vary crystallization characteristics.

Recent advances in solution-phase deposition of semiconductor films for thin-film transistor applications have demonstrated that chalcogenide materials with very little organic contamination can be prepared from soluble hydrazine-based precursors at low process temperatures (less than 400 °C)[7,9]. A bulk metal chalcogenide is dissolved in the reducing solvent hydrazine and reacts with additional chalcogen to form a soluble precursor, which can be used to prepare thin films of the original chalcogenide material. These hydrazine-based precursors show minimal mass loss on thermal conversion, which favours continuous, high-quality inorganic films. Furthermore, binary metal chalcogenide precursors can be combined in solution to prepare more complex film compositions, for example the ternary semiconductors $CuInSe_2$ and $CuInTe_2$ (refs 6,8).

To explore solution routes to GeSbSe phase-change materials, soluble Ge–Se and Sb–Se precursors were prepared from bulk GeSe and Sb_2Se_3, respectively, by dissolving the metal chalcogenide in hydrazine in the presence of additional elemental selenium. Removing the hydrazine, we recover solid precursors, which can be redissolved to process into thin films. Thermal gravimetric analysis of the precursor powders (see Supplementary Information, Fig. S1) indicates that decomposition is essentially complete by 160 °C, and Rutherford backscattering spectrometry (RBS) analysis of precursor powders and thin films annealed at or above this temperature detected no residual nitrogen within a detection limit of about 5%. Continuous GeSbSe thin films were deposited by spin coating onto clean silicon wafers from a dimethylsulphoxide/ethanolamine solution, then annealing to remove the solvents and decompose the precursors.

Thin films deposited from the Sb–Se precursor are crystalline as prepared and remain so on heating, their diffraction pattern corresponding to orthorhombic Sb_2Se_3 (Fig. 1a). Conversely, the Ge–Se precursor yields amorphous thin films, which remain amorphous on thermal annealing up to more than 400 °C (Fig. 1d), consistent with the well-known glass-forming properties of $GeSe_x$ materials[19,20]. Intermediate phase-change behaviour can be achieved by blending the Sb–Se and Ge–Se precursors in the casting solution. A few molar per cent of Ge doped into an $SbSe_x$ film is sufficient to yield an amorphous film that then crystallizes on annealing at 200−250 °C. Increasing the degree of Ge doping systematically increases the crystallization temperature in this range (Fig. 1b,c) until no crystallization is observed above 15% Ge for temperatures up to around 450 °C. In all cases, the diffraction
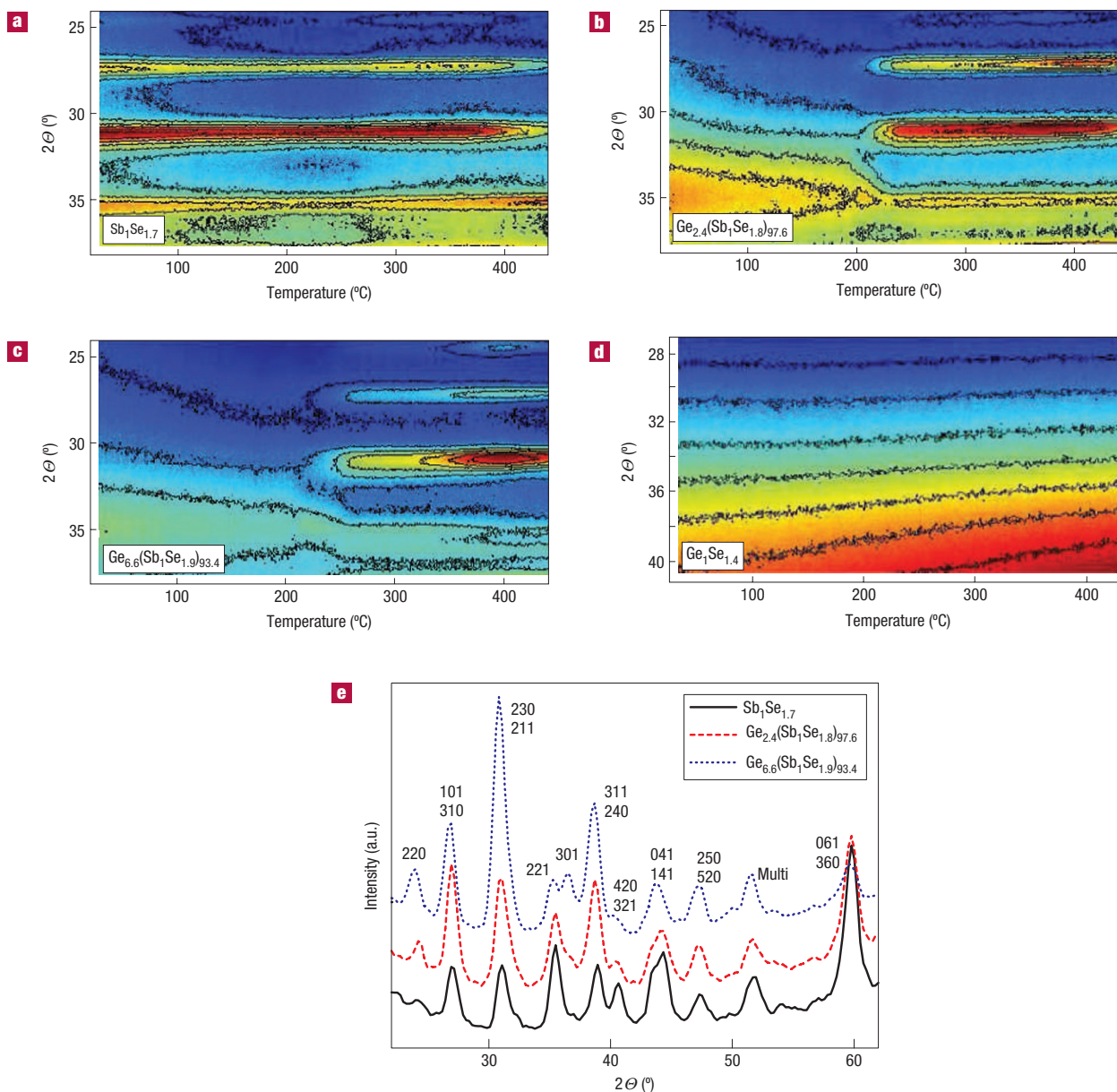
Figure 1 X-ray diffraction of GeSbSe thin films during thermal annealing. Film compositions determined by RBS are indicated for each frame. **a**, Ge-free SbSe film; **b,c**, films with increasing Ge doping level; **d**, GeSe film. **e**, Films with no or low levels of Ge doping crystallize in an orthorhombic structure, indexed to Sb_2Se_3 (15-0861). Data have been offset for clarity.

pattern of the crystallized films could be assigned to orthorhombic Sb_2Se_3, with no significant dependence of lattice constant on the Ge doping level, though slight textural differences are apparent in the peak intensities (Fig. 1e). Electrical readout in PCRAM devices is based on the contrast in resistivity between the amorphous and crystalline phases. The resistivity of a GeSbSe film drops sharply at a temperature consistent with the range of the crystallization temperatures observed by X-ray diffraction (see Supplementary Information, Fig. S2), indicating the potential for reading spin-on phase-change materials electrically.

Laser-pulse annealing[12,21] was used to further characterize the amorphous–crystalline phase change in GeSbSe thin films. Films were deposited on silicon wafers precoated with 40 nm of sputtered Al_2O_3 to serve as a partial thermal barrier between the film and the substrate. Laser-pulse power and duration were varied, and change in reflectivity was used as an indication of crystallization to map the crystallization of amorphous as-prepared GeSbSe films (Fig. 2a). As with other chalcogenide phase-change materials such as $Ge_2Sb_2Te_5$ and $SbSe_x$, we expect an increase in optical reflectivity to accompany crystallization. Pulse lengths of around 3 µs, the apparent minimum crystallization time for the as-prepared film, were sufficient to increase the reflectivity by a few per cent. When a phase-change film is first initialized to the crystalline state, by heating above its crystallization temperature, isolated areas can be switched back to the amorphous state[21]. Laser pulses can melt the phase-change material, which is then quenched to the amorphous state by rapid heat transfer through the thermal-barrier material to the silicon substrate. A GeSbSe
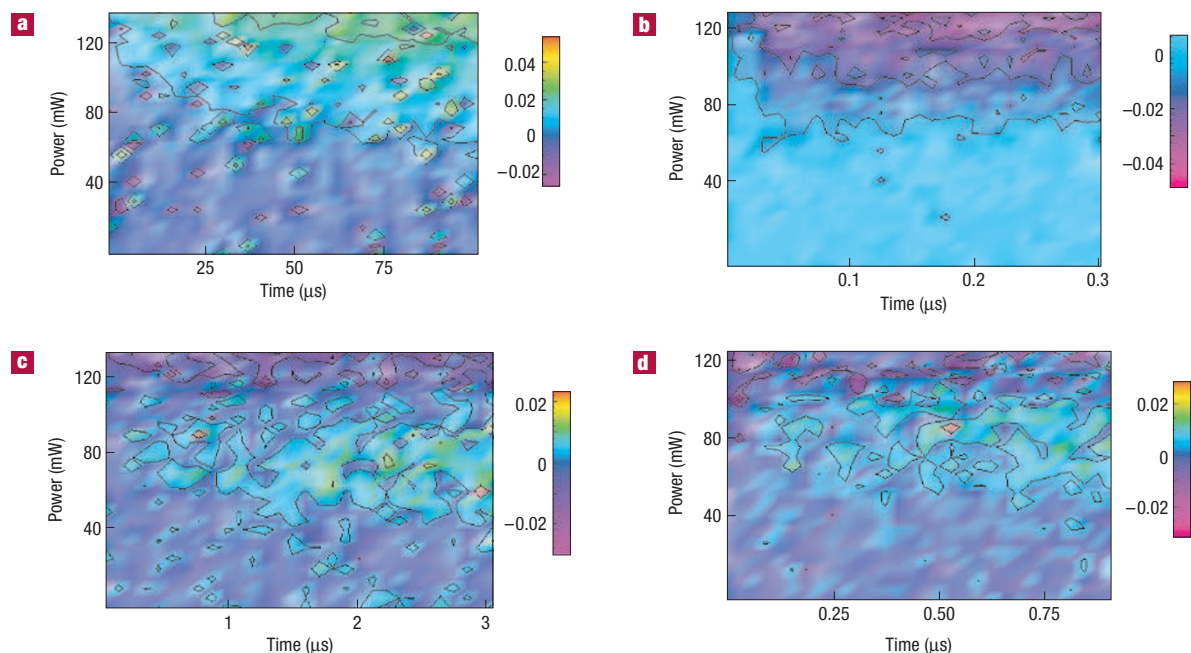
Figure 2 Laser-pulse annealing of GeSbSe thin films. **a**, An amorphous, as-prepared film of GeSbSe is heated using laser pulses of varied time and power. A map of the change in reflectivity of the heated spots indicates local crystallization of the film above about 60 mW (for longer pulses) and 3 μs (for higher-powered pulses). **b**, A GeSbSe film is first thermally crystallized then covered by a protective Al_2O_3 capping layer. Brief laser pulses above about 80 mW induce a drop in reflectivity, indicating the phase-change film has been melt-quenched to the amorphous state. **c**, Melt-quenched amorphous spots switch back to the crystalline state, shown by enhanced reflectivity, after applying a second pulse. A 130 mW, 300 ns prepulse amorphizes the spot and a second variable pulse is applied to recrystallize it. **d**, Pulses as short as 100–150 ns are sufficient to yield a measurable reflectivity enhancement. The scale to the right of each frame indicates fractional change in reflectivity.

film was annealed for 10 min at 300 °C to crystallize the material, then capped with 20 nm of sputtered SiO_2 to protect it from oxidation or evaporation at the high temperatures achieved during the melt-quench process. The initial reflectivity of this capped sample is reduced by about one-third, consistent with greater absorption of the laser, so the effect of a given-power laser pulse cannot be directly compared for the two samples. The optical signature of amorphization due to melt-quench is a decrease in reflectivity, which is observed to decrease by a few per cent for the GeSbSe film (Fig. 2b). Melt-quench occurs at the same power as crystallization of the uncapped as-prepared sample, consistent with greater absorbed power in the capped sample, but also possibly related to a difference in thermal properties of the films themselves. Finally, the film can be recrystallized by following the melt-quench pulse with a somewhat lower-power crystallization pulse. The reflectivity increases, indicating switching back to the crystalline phase (Fig. 2c). Enhanced reflectivity is observed down to 100–150 ns pulses (Fig. 2d), indicating very rapid crystallization of the melt-quenched material. Such differences between the crystallization kinetics of as-prepared and melt-quenched phase change material have been previously observed, and identifying them is essential to designing data-storage devices, which switch between the melt-quenched and crystallized states[13,22,23]. Enhanced local order in the amorphous phase can be produced in different ways, such as by crystallization and subsequent melt-quenching or by exposing the amorphous material to a short laser pulse that is not long enough to crystallize the material[13,22,23]. In each case, this greater local order has been correlated to much faster crystallization of the still-amorphous material compared with the as-deposited material[13,22,23]. Furthermore, crystallization of the as-deposited material requires both the formation of nuclei

of critical size and their subsequent growth via propagation of the crystalline–amorphous boundary, whereas crystallization of a melt-quenched spot may occur via growth from the boundary alone.

Solution processing of phase-change material is not only a low-cost, simple alternative to sputter deposition—it also offers potential advantages for patterning and eventual fabrication of PCRAM devices. It is advantageous, to minimize the current required to reset a PCRAM device, to contain the phase-switching material in a through hole within an insulating material. However, fabricating such a structure requires either depositing material into a preformed hole or etching the material, then surrounding it with the insulator. The first option poses a difficult challenge for sputter deposition, which struggles to fill such holes, particularly at small sizes and/or aspect ratios greater than unity, without forming 'keyhole' voids[24]. Etching is also an unsatisfying option as it adds complexity and poses the risk of unacceptable damage to the phase-change material. During solution-phase deposition, however, capillary forces drive the solution into prepatterned holes or vias, depositing the precursor, which is then decomposed to phase-change material. Drop casting a precursor solution onto a silicon oxide film patterned with 2:1-aspect-ratio vias completely fills these vias with GeSbSe after thermal annealing to decompose the precursors (Fig. 3a). Even nanoscale patterns can be easily formed through straightforward solution deposition. For example, a large array of nanoscale dots of GeSbSe was formed on a silicon substrate using a block-copolymer template. The template is generated by self-assembly of a poly(styrene)–poly(methylmethacrylate) (PS-*b*-PMMA) block copolymer and consists of an array of holes in a polystyrene matrix (Fig. 3b)[25,26]. Following self-assembly of the block-copolymer film, the PMMA is displaced with acetic acid, leaving an array of nanoscale

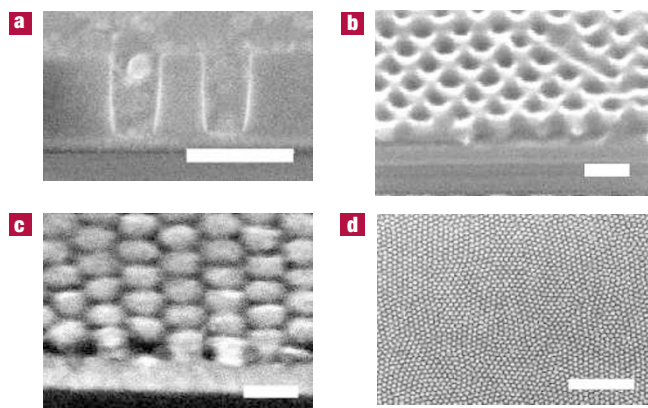**Figure 3 Filling patterns with phase-change material. a**, Drop casting a Ge–Sb–Se precursor solution completely fills preformed high-aspect-ratio vias (in thermal silicon oxide) with GeSbSe phase-change material. **b**, A PS mesh with an array of about-30-nm-diameter cylindrical holes is formed by developing a self-assembled thin film of the block copolymer PS-*b*-PMMA. **c,d**, An array of GeSbSe nanodots is formed by solution deposition and lift-off of the PS mesh. The scale bars are 500, 50, 50 and 500 nm, respectively.

holes[26]. Then, the bottoms of the holes are cleared down to the substrate using a 5 s oxygen plasma etch to remove the underlying random copolymer layer[25]. The plasma etch also leaves the template hydrophilic, which facilitates deposition of the phase-change precursor. The template is filled with precursor by spin casting, then annealed to form an array of ∼30 nm diameter GeSbSe nanodots on the silicon surface. Finally, the nanopattern is exposed by lift-off of the PS template with toluene, which removes any superficial GeSbSe (Fig. 3c,d). The GeSbSe nanodots are amorphous as prepared and crystallize on thermal annealing to the same orthorhombic structure as observed in the blanket films (Fig. 4). For films prepared from the same precursor solution, the nanodot array crystallizes at more than 35 °C lower temperature than the blanket film. Elemental analysis of the films by particle-induced X-ray emission (PIXE) analysis reveals that the nanodot array is actually richer in Ge than the blanket film (film, $Ge_{2.8}Sb_{32.3}Se_{64.9}$; nanodot array, $Ge_{5.6}Sb_{31.0}Se_{63.4}$), apparently owing to differences in precursor decomposition in the two geometries. (PIXE was used for elemental analysis of these samples because the overlap of the Ge and Se peaks in RBS made it difficult to accurately ascertain their Ge content.) The effective reduction in the crystallization temperature is therefore even greater than it seems, because additional Ge increases the transition temperature for the blanket films. The temperature difference could be due to the reduced volume of the crystallizing material, the greater interfacial area or a combination of factors[27]. A reduction in crystallization temperature for nanosized phase-change islands, fabricated by electron-beam lithography, has also been observed (S.R. *et al.*, unpublished). Identifying and controlling such effects will be essential to successful scaling of PCRAM into the nanoscale regime. Nanopatterning of solution-deposited material provides a simple test bed for further investigation of such phenomena.

We have demonstrated a versatile, solution-based, low-temperature approach to the deposition of chalcogenide phase-change materials. Our approach is made on the basis of the synthesis of soluble precursors, which can be combined to tune the composition and properties of the final material. Spin-on GeSbSe films show a tuneable crystallization temperature in the range of 200−250 °C and a minimum crystallization time of the
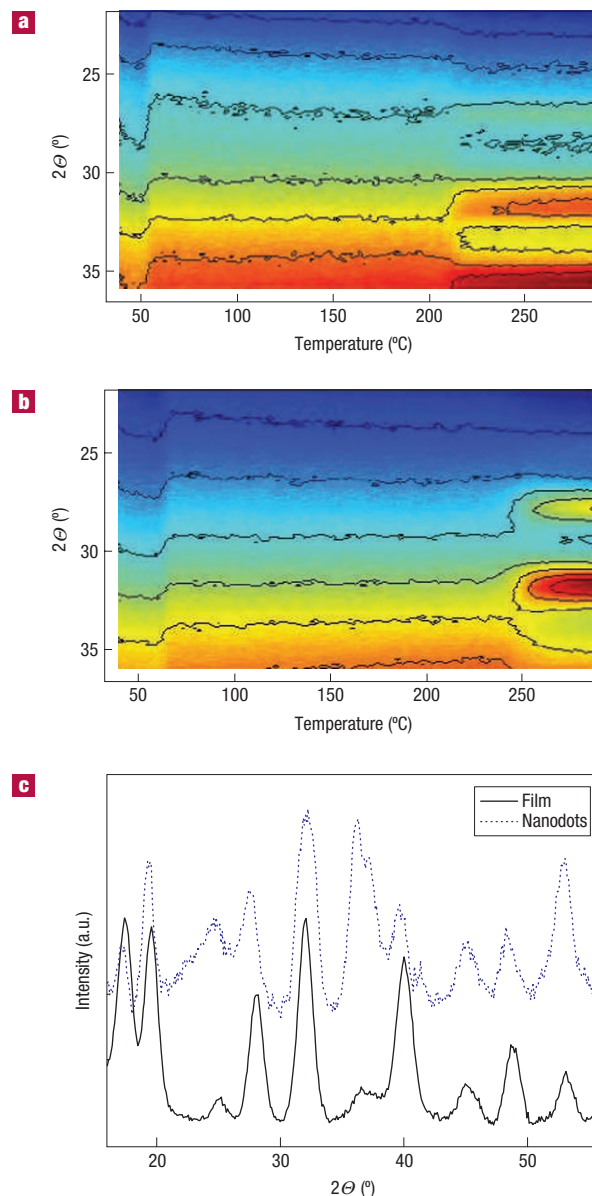

Figure 4 X-ray diffraction of GeSbSe nanodot array during thermal annealing. a,b, A nanodot array as shown in Fig. 3, capped with 10 nm SiO_2 to protect the large-surface-area pattern (**a**), crystallizes on thermal annealing at a temperature more than 35 °C lower than a SiO_2-capped blanket film (**b**). **c**, The diffraction pattern of the crystallized nanodots reflects the same orthorhombic structure as the thin film.

order of 100 ns for melt-quenched material. We consider these results to be a promising indication that this process is capable of yielding materials of practical use for phase-change data storage. Solution deposition also enables facile filling of high-aspect-ratio vias, offering a potential advantage in device fabrication over conventional sputter-deposition methods. Hole filling has also been leveraged to produce arrays of GeSbSe nanodots around 30 nm in diameter, which crystallize at a reduced temperature when compared with a blanket film.

Note added in proof: A hydrazine solution route to films of KSb_5S_8 was also recently reported. This material undergoes an amorphous to crystalline phase transition on the timescale of seconds (ref. 28).

METHODS

PRECURSOR SYNTHESIS AND CHARACTERIZATION

All chemicals were purchased from Aldrich and used as received unless otherwise noted. The Sb–Se precursor was prepared by combining 1 mmol (480 mg) Sb_2Se_3 with 2 mmol (158 mg) Se in 1 ml freshly distilled hydrazine and stirring at room temperature in an inert atmosphere for one week. The dark-coloured solution was filtered to remove any undissolved solids then dried under flowing nitrogen to a brown solid. The Ge–Se precursor was prepared similarly by combining 1 mmol (152 mg) GeSe and 1 mmol (79 mg) Se in 1 ml hydrazine. The dry product was a deep-red solid. Decomposition of the precursors was characterized by thermal gravimetric analysis under flowing dry nitrogen at a heating rate of $2\,°C\,min^{-1}$.

PREPARATION OF THIN FILMS

Substrates were cleaned using a Piranha process (3:1 H_2SO_4 to H_2O_2) then transferred to an inert atmosphere. Precursor solutions were prepared by stirring $40\,mg\,ml^{-1}$ of the solids in mixed 5:3-volume-ratio dimethylsulphoxide to ethanolamine solvent at room temperature overnight to form clear orange solutions, which were then filtered to remove any undissolved solids. The solutions were combined to the desired composition then spin coated. Samples were placed on a hotplate held at $100\,°C$ for 3 min to dry, then held at $180\,°C$ for 20 min to finish decomposition of the precursors. Thicker, drop-cast films were held at $100\,°C$ for one hour and $180\,°C$ for five hours.

Block-copolymer templates were prepared using PS-*b*-PMMA and PS–PMMA random copolymer from Polymer Source by a previously described process[26]. Following development with glacial acetic acid, the template was etched with a mild isotropic oxygen plasma (30 s.c.c.m. O_2, 6 mtorr, 300 mW inductively coupled plasma). The phase-change material was spin cast following the same procedure as used for thin films, except that the concentration of precursor was $20\,mg\,ml^{-1}$. Lift-off was accomplished by sonicating in toluene for 30 min.

X-RAY DIFFRACTION OF THIN FILMS

X-ray diffraction was carried out at the National Synchrotron Light Source at Brookhaven National Laboratory using beamline X20C with radiation of wavelength 1.797 Å. The beamline is equipped with a high-throughput synthetic multilayer monochromator and a linear diode array detector, which was used to record the diffracted peak intensities over a 2Θ range of 15°. The range was selected according to the position of the strongest diffraction peaks. Samples were heated at a rate of $1\,°C\,s^{-1}$ in a purified helium atmosphere using a boron nitride heater.

LASER-PULSE ANNEALING

Films of phase-change material were heated with a pulsed 514 nm laser beam of up to 150 mW power, focused to $1.1\,\mu m$ $1/e^2$ diameter. The reflectivity of the film was monitored with a continuous probe beam at 633 nm of power 0.7 mW focused to $1.0\,\mu m$ $1/e^2$ diameter and coincident with the pulsed beam. The intensity of the reflected probe beam was recorded with a digital oscilloscope. The system response time due to detector rise time and pulsed beam rise time is about 10 ns. The results in Fig. 2a,b were obtained by varying the power and pulse duration of the pulsed beam while translating the sample a few micrometres between each pulse exposure . The oscilloscope traces were analysed to obtain the initial (R_i) and final reflectivity (R_f) of the film, and contours of $(R_f-R_i)/R_i$ were plotted to obtain the figure. Recrystallization of melt-quenched spots was achieved by applying a pulse sufficient to amorphize the film followed by a second pulse of variable length and power at the same location. The change in reflectivity due to the second pulse is plotted in Fig. 2c,d.

References

1. Mansuripur, M. Rewritable optical disk technologies. *Proc. SPIE* **4109**, 162–176 (2000).
2. Yamada, N. Erasable phase-change optical materials. *Mater. Res. Soc. Bull.* **21**, 48–50 (1996).
3. Lankhorst, M. H. R., Ketelaars, B. W. S. M. M. & Wolters, R. A. M. Low-cost and nanoscale non-volatile memory concept for future silicon chips. *Nature Mater.* **4**, 347–352 (2005).
4. Ovshinsky, S. R. Reversible electrical switching phenomena in disordered systems. *Phys. Rev. Lett.* **21**, 1450–1453 (1968).
5. Hudgens, S. & Johnson, B. Overview of phase-change chalcogenide nonvolatile memory technology. *Mater. Res. Soc. Bull.* **29**, 829–832 (2004).
6. Milliron, D. J., Mitzi, D. B., Copel, M. & Murray, C. E. Solution processed metal chalcogenide films for p-type transistors. *Chem. Mater.* **18**, 587–590 (2006).
7. Mitzi, D. B., Copel, M. & Chey, S. J. Low-voltage transistor employing a high-mobility spin-coated chalcogenide semiconductor. *Adv. Mater.* **17**, 1285–1289 (2005).
8. Mitzi, D. B., Copel, M. & Murray, C. E. High-mobility p-type transistor based on a spin-coated metal telluride semiconductor. *Adv. Mater.* **18**, 2448–2452 (2006).
9. Mitzi, D. B., Kosbar, L. L., Murray, C. E., Copel, M. & Afzali, A. High-mobility ultrathin semiconducting films prepared by spin coating. *Nature* **428**, 299–303 (2004).
10. Kolobov, A. V. *et al.* Understanding the phase-change mechanism of rewritable optical media. *Nature Mater.* **3**, 703–708 (2004).
11. Welnic, W. *et al.* Unravelling the interplay of local structure and physical properties in phase-change materials. *Nature Mater.* **5**, 56–62 (2006).
12. Kang, M. J. *et al.* Structural transformation of Sb_xSe_{100-x} thin films for phase change nonvolatile memory applications. *J. Appl. Phys.* **98**, 014904 (2005).
13. Wuttig, M. *et al.* The quest for fast phase change materials. *J. Magn. Magn. Mater.* **249**, 492–498 (2002).
14. von Pieterson, L., Lankhorst, M. H. R., van Schijndel, M., Kuiper, A. E. T. & Roosen, J. H. J. Phase-change recording materials with a growth-dominated crystallization mechanism: A materials overview. *J. Appl. Phys.* **97**, 083520 (2005).
15. Babeva, T., Dimitrov, D., Kitova, S. & Konstantinov, I. Optical properties of phase-change optical disks with Sb_xSe_{100-x} films. *Vacuum* **58**, 496–501 (2000).
16. Dimitrov, D., Ollacarizqueta, M. A., Afonso, C. N. & Starbov, N. Crystallization kinetics of Sb_xSe_{100-x} thin films. *Thin Solid Films* **280**, 278–283 (1996).
17. Barton, R., David, C. R., Rubin, K. & Lim, G. New phase change material for optical recording with short erase time. *Appl. Phys. Lett.* **48**, 1255–1257 (1986).
18. El-Salam, F. A., Afify, M. A. & El-Wahabb, E. A. Switching phenomenon in amorphous Sb_2Se_3. *Vacuum* **44**, 17–22 (1993).
19. Katti, V. R., Govindacharyulu, P. A. & Bose, D. N. Electrical and optical properties of amorphous semiconducting GeSe and GeSbSe films. *Thin Solid Films* **14**, 143–148 (1972).
20. Salmon, P. S. & Petri, I. Structure of glassy and liquid $GeSe_2$. *J. Phys. Condens. Matter* **15**, S1509–S1528 (2003).
21. Weidenhof, V., Pirch, N., Friedrich, I., Ziegler, S. & Wuttig, M. Minimum time for laser induced amorphization of $Ge_2Sb_2Te_5$ films. *J. Appl. Phys.* **88**, 657–664 (2000).
22. Coombs, J. H., Jongenelis, A. P. J. M., Vanesspiekman, W. & Jacobs, B. A. J. Laser-induced crystallization phenomena in GeTe-based alloys. 1. Characterization of nucleation and growth. *J. Appl. Phys.* **78**, 4906–4917 (1995).
23. Weidenhof, V., Friedrich, I., Ziegler, S. & Wuttig, M. Laser induced crystallization of amorphous $Ge_2Sb_2Te_5$ films. *J. Appl. Phys.* **89**, 3168–3176 (2001).
24. Sandhu, G. S. Process technology and integration challenges for high performance interconnects. *Thin Solid Films* **320**, 1–9 (1998).
25. Guarini, K. W., Black, C. T., Milkove, K. R. & Sandstrom, R. L. Nanoscale patterning using self-assembled polymers for semiconductor applications. *J. Vac. Sci. Technol.* **19**, 2784–2788 (2001).
26. Xu, T. *et al.* Block copolymer surface reconstruction: A reversible route to nanoporous films. *Adv. Funct. Mater.* **13**, 698–702 (2003).
27. Martens, H. C. F., Vlutters, R. & Prangsma, J. C. Thickness dependent crystallization speed in thin phase change layers used for optical recording. *J. Appl. Phys.* **95**, 3977–3983 (2004).
28. Mitzi, D. B. *et al.* Solution-based processing of the phase-change material KSb$_5$S$_8$. *Chem. Mater.* **18**, 6278–6282 (2006).

Author contributions

D.J.M. developed the GeSbSe materials and prepared all GeSbSe samples, D.J.M. and S.R. made electrical measurements, S.R. and J.J.S. collected and analysed XRD data, R.M.S. carried out and interpreted laser pulse annealing experiments.